The American Journal of Human Genetics, Volume *91*

Supplemental Data

Autosomal-Recessive Congenital Cerebellar Ataxia Is Caused by Mutations in Metabotropic Glutamate Receptor 1

Velina Guergueltcheva, Dimitar N. Azmanov, Dora Angelicheva, Katherine R. Smith, Teodora Chamova, Laura Florez, Michael Bynevelt, Thai Nguyen, Sylvia Cherninkova, Veneta Bojinova, Ara Kaprelyan, Lyudmila Angelova, Bharti Morar, David Chandler, Radka Kaneva, Melanie Bahlo, Ivailo Tournev, and Luba Kalaydjieva

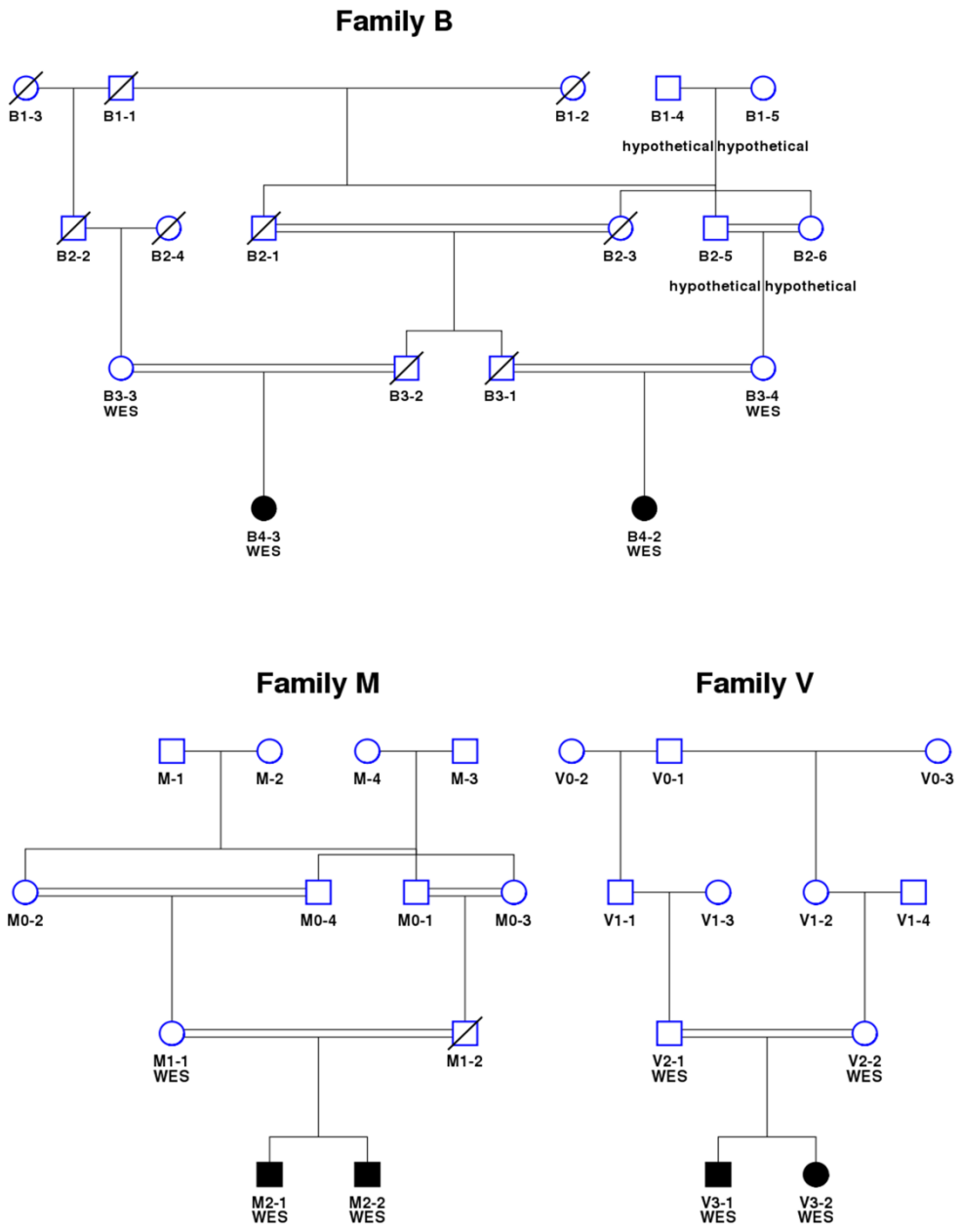

Figure S1. Pedigree Structures of the Families as Used in the Linkage Analysis

For the linkage analysis, hypothetical consanguinity loops were added to account for the undocumented consanguinity detected by the inbreeding analysis (inbreeding coefficients shown in Table S2). WES – whole exome sequencing

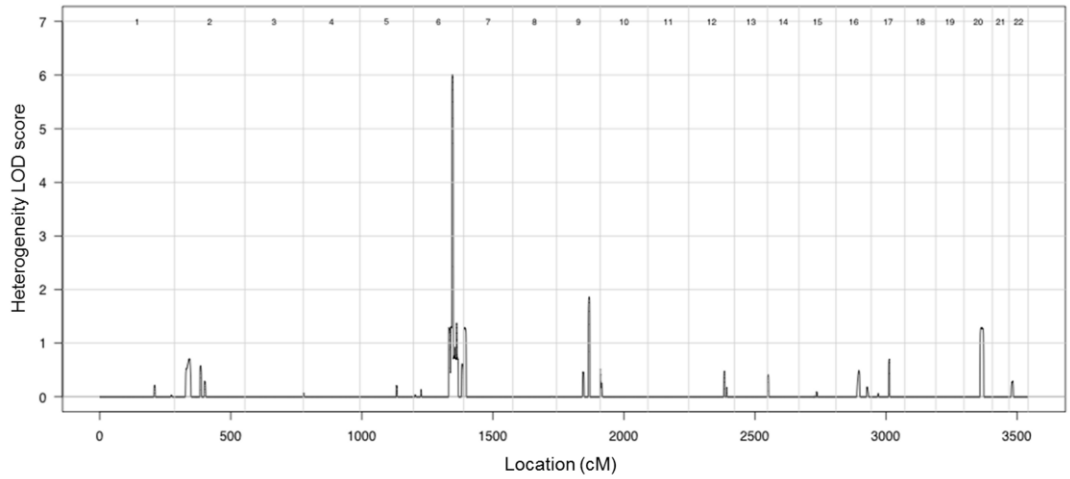

Figure S2. Multipoint Parametric Linkage Analysis in Families V, M, and B

The analysis was conducted using SNP genotypes extracted from the exome sequencing data, under a fully penetrant autosomal recessive model, 0% phenocopy rate, disease allele frequency 0.00001. The chromosome 6q24 region was the only one where all three families contributed to the linkage peak. Gridlines on the X axis delineate chromosomes from 1 to 22.

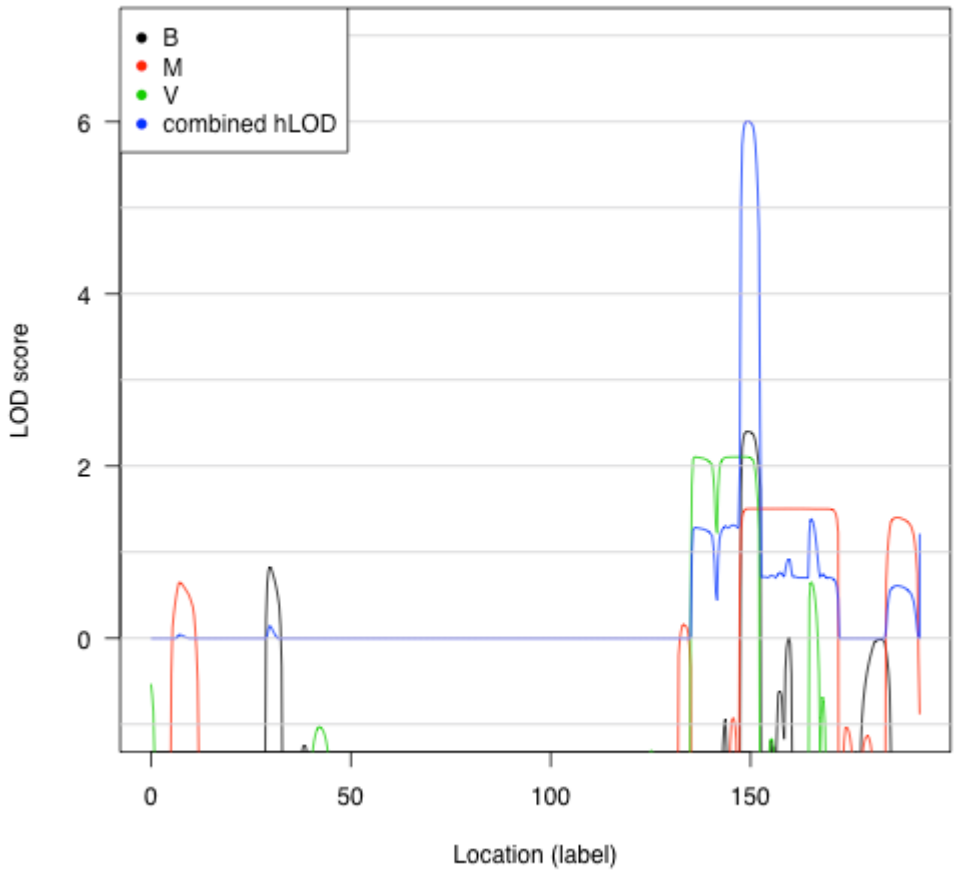

Figure S3. Contribution of Each of the Three Families (V, M, and B) to the Overall Heterogeneity LOD Score on Chromosome 6q24

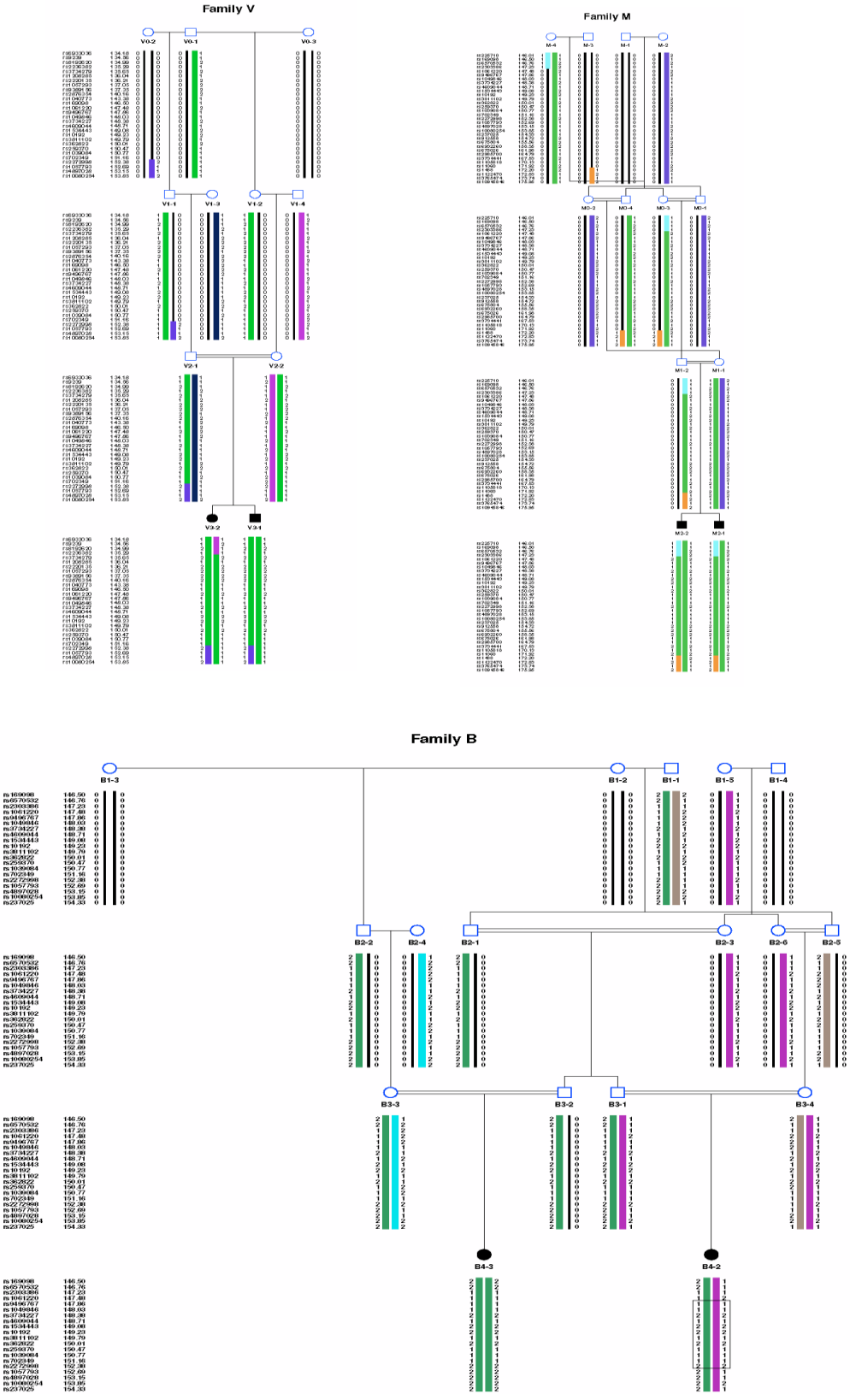

Figure S4. Inferred Haplotypes in the Linked 6q24 Region for Families V, M, and B, Examined Using HaploPainter (Thiele and Nürnberg 2005)

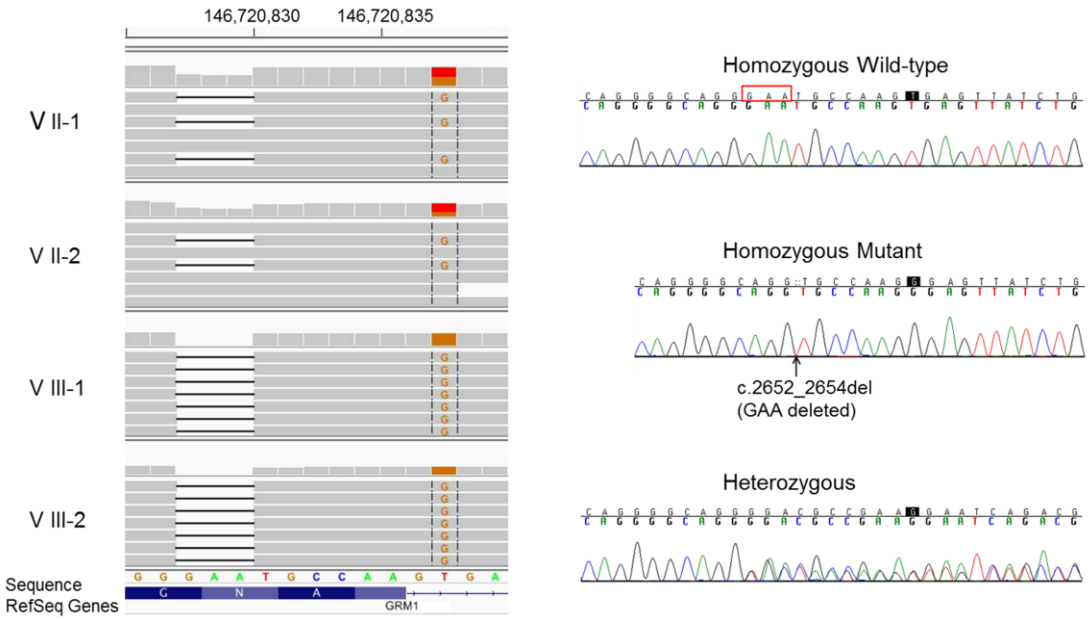

Figure S5. Tandem *GRM1* Mutations Identified by Exome Sequencing

Left panel: Integrative Genomics Viewer snapshot of the short reads alignment from the exome sequencing of family V. The 3bp c.2652_2654del deletion is shown as a gap, the c.2660+2T>G mutation, is in orange, boxed. Nucleotide positions follow the hg19 reference genome. Right panel: Verification of the mutations by Sanger sequencing. PCR amplification and sequencing were done with primers 5'-ACTATGCCTTCAAGACCCGC-3' and 5'-GGGGAAATGGAAGAGACAAC-3'. On the chromatograms, c.2652_2654del is boxed in the wild-type and its position indicated with an arrow in the mutant sequence; c.2660+2T>G is highlighted. In heterozygotes, c.2652_2654del is unambiguously detected, while c.2660+2T>G is masked on the forward strand (shown) by the deletion, and on the reverse strand by an intronic repeat starting 20 bp downstream. Its presence was confirmed by pyrosequencing (Suplemental Figure S7).

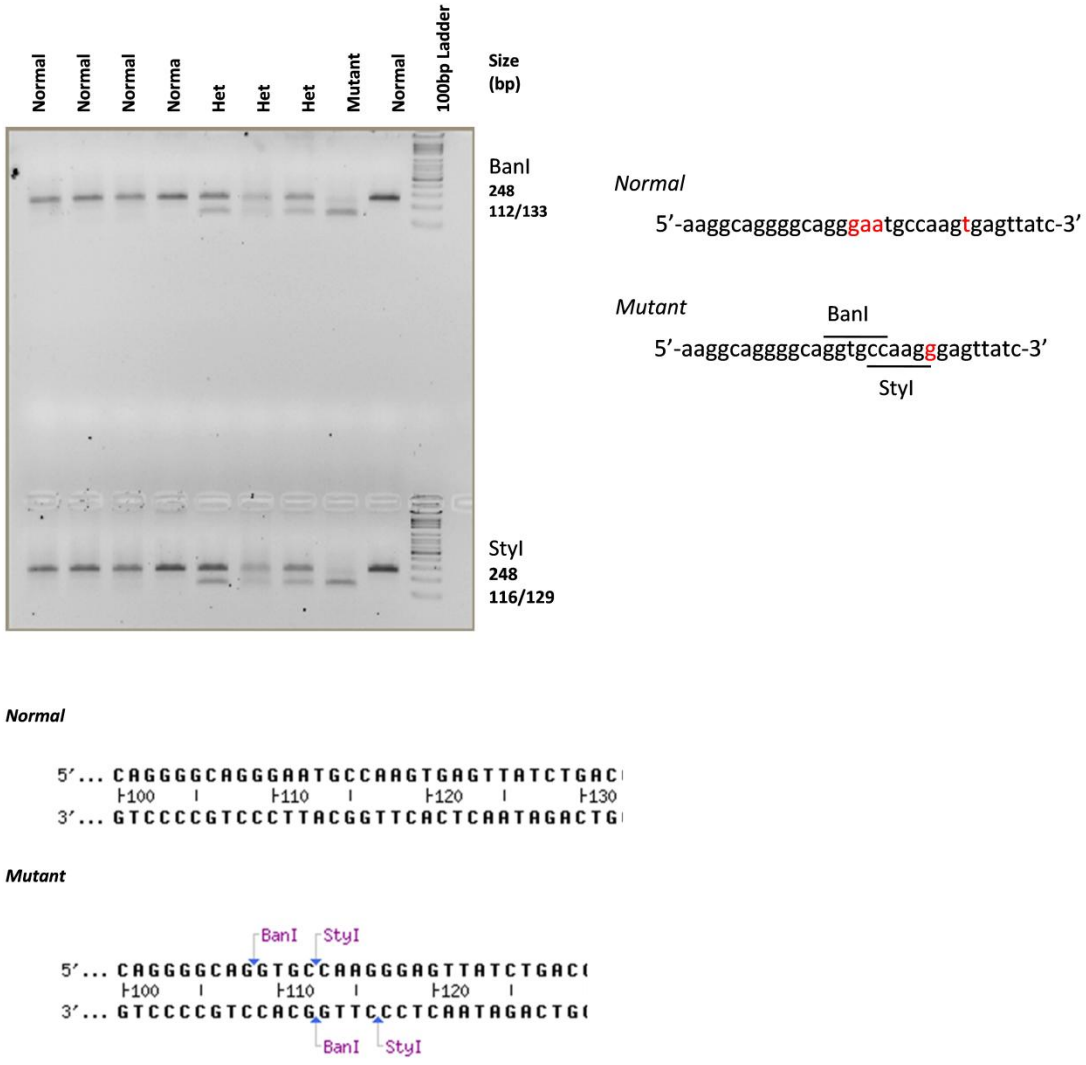

Figure S6. PCR-Based RFLP Assays Designed to Detect Independently the Two *GRM1* Mutations in Heterozygous Individuals

A 248 bp fragment (hg19 chr6:146720718-146720965) was PCR-amplified with primers 5'-GTGCCTTCACCACCTCTGAT-3' and 5'-GGGGAAATGGAAGAGACAAC-3'. BanI was used for the detection of GRM1 c.2652_2654del, and StyI for GRM1 c.2660+2T>G. Restriction digestion was performed following the manufacturer's protocols (NEB, Ipswich, MA, USA). The fragments were separated by agarose gel electrophoresis. Positive results were confirmed by pyrosequencing.

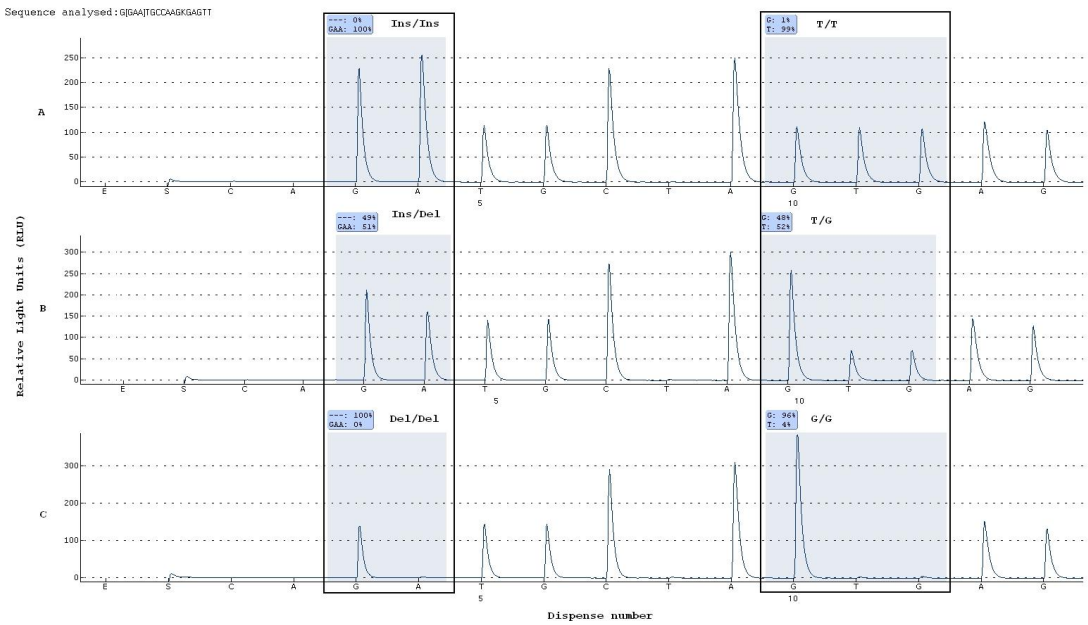

Figure S7. Pyrosequencing as a Confirmatory Test for the Presence of the Mutations

Pyrograms of A) unaffected control, B) heterozygote carrier and C) ataxia patient. Peak heights are shown as relative light units detected for nucleotide dispensed. The heights at variable sites are compared to those generated by surrounding known sequence to determine the sequence at the variable site. At the c.2652_2654del mutation site, the height of the G and A peaks decreases in mutation heterozygotes and further in homozygotes. For the c.2660+2T>G mutation, heterozygosity and homozygosity for the mutant G allele results in increasing peak height, representing a sequence of three consecutive Gs at dispense 10.

A 258 base pair segment containing the mutated sites was PCR amplified (primers and conditions in the table below). A biotin-labeled primer (IDT) was used to purify the final PCR product using Sepharose beads. The PCR product was bound to Streptavidin Sepharose High Performance beads (GE Healthcare Life Sciences, Rydalmere, NSW, Australia), and the sepharose beads containing the immobilized PCR product were denatured, and washed using proprietary solutions (Qiagen, Doncaster, Vic, Australia) on the Pyrosequencing Vacuum Prep Tool (Qiagen). 0.3 µM of pyrosequencing primer was annealed to the purified single-stranded PCR product. Pyrosequencing was performed on a PyroMark 24 Pyrosequencing System (Qiagen). Data analysis was performed using the PyroMark Q24 software.

Pyrosequencing primers

Primer name	Sequence	Modification/purification
GRM1_F	GTG CCT TCA CCA CCT CTG ATG	Standard Desalting
GRM1_R	/5Biosg/GGG GAA ATG GAA GAG ACA ACT	5' Biotin/ HPLC Purification
GRM1_S	AGA AGG CAG GGG CAG	Standard Desalting

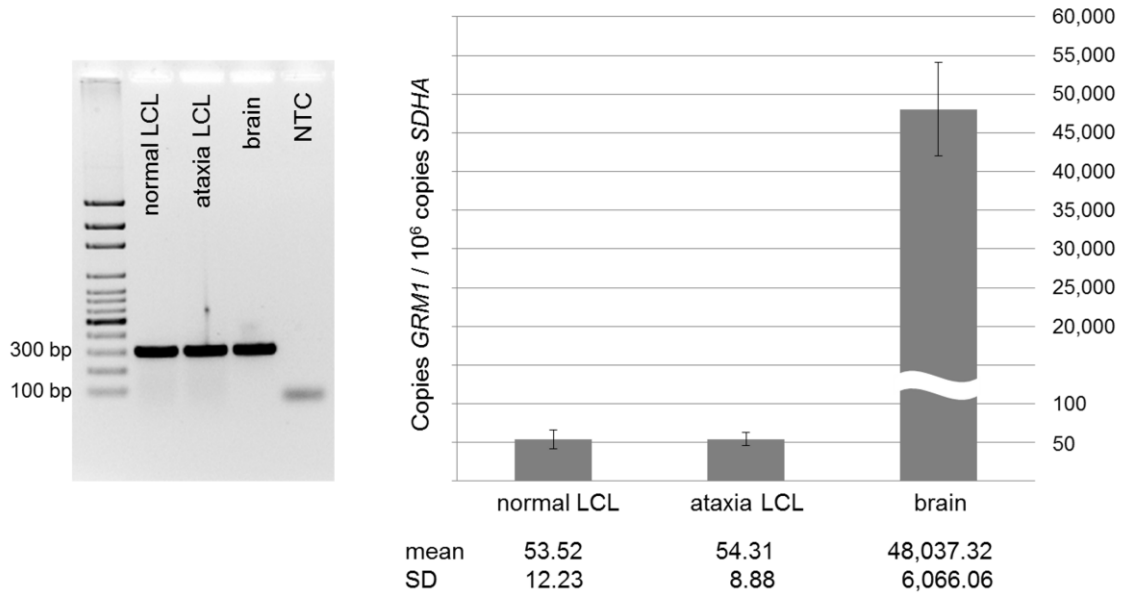

Figure S8. *GRM1* Expression Levels in Control and Ataxia LCLs

Left panel: Agarose gel electrophoresis of RT-PCR products obtained with primers targeting invariable upstream exons3-4 (expected fragment size 304bp). Right panel: *GRM1* transcript abundance relative to endogenous *SDHA* expression.[1] Standards (3 to 300,000 copies) were prepared by serial dilutions of the RT-PCR products from normal LCLs, after concentration measurements with the Quant-iT PicoGreen dsDNA kit (Life Technologies, Mulgrave, Vic, Australia) and product size conversions to the mass of a single copy.[2] Quantitative PCR (in triplicates), was done with iQ SYBR Green Supermix (BioRad, Gladesville, NSW, Australia). Standard curves were generated by plotting the average Ct values versus the log-transformed input copies of the standards (R^2>0.99). The number of copies in test samples was interpolated using the linear regression formula.

1. Hruz, T., Wyss, M., Docquier, M., Pfaffl, M.W., Masanetz, S., Borghi, L., Verbrugghe, P., Kalaydjieva, L., Bleuler, S., Laule, O., et al. (2011). RefGenes: identification of reliable and condition specific reference genes for RT-qPCR data normalization. BMC Genomics *12*, 156.

2. Pfaffl, M.W. (2004). Quantification strategies in real-time PCR. In IUL Biotechnology Series: A-Z of quantitative PCR, S.A. Bustin, ed. (La Jolla: International University Line), pp. 87-112.

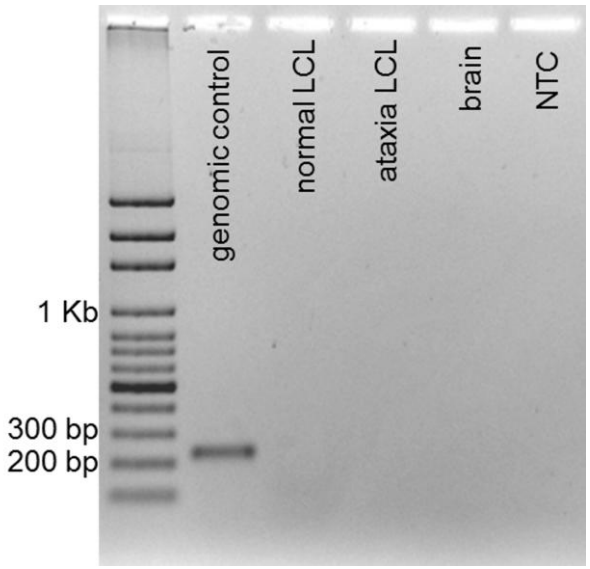

Figure S9. Control PCR Testing for Genomic DNA Contamination of the RNA Samples Used in the RT-PCR Amplifications

The forward primer is in *GRM1* exon 7, the reverse primer is in intron 7, and the expected product for gDNA is 231 bp (Table S4).

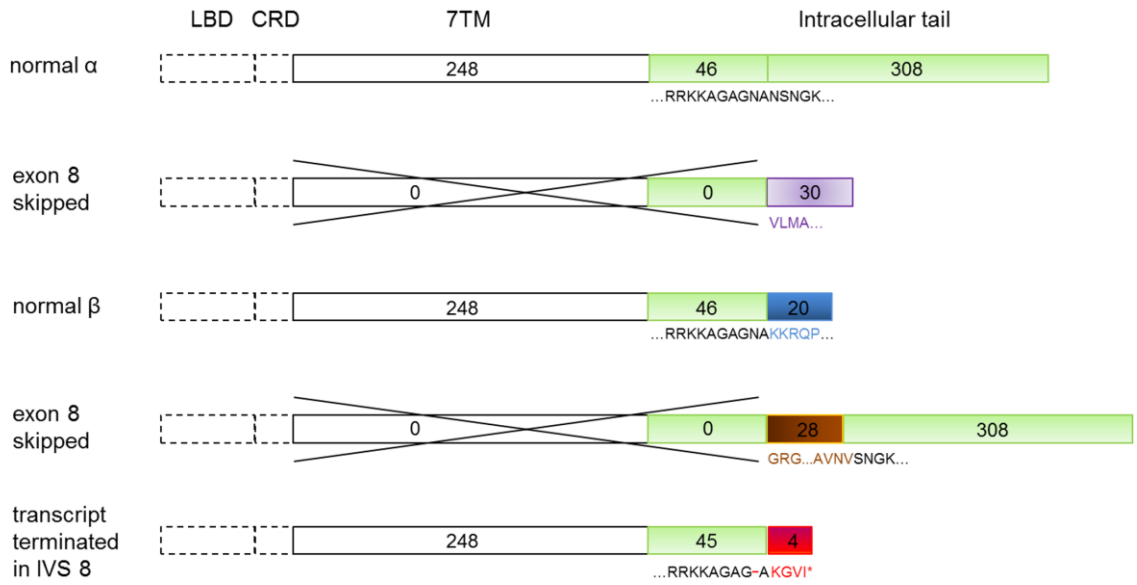

S10. mGluR1α and mGluR1β1 Protein Domains and Predicted Products of the Aberrant Transcripts Observed in Ataxia LCLs

The receptor domains and corresponding numbers of constituent amino acid (AA) in the nomal mGluR1α and mGluR1β1 isoforms are as shown in UniProt Accession number Q13255. Predictions of the products of experimentally observed aberrant transcrips were obtained using the Expasy Translate Tool. Different colours are used to highlight differences in the intracellular tail, with a small number of AA residues shown in the critical regions affected by the mutation. The vertical line in the tail delineates the parts encoded by exon 8 and downstream exons. Exon 8 skipping is predicted to lead to receptor molecules missing the conserved transmembrane domain. In addition, exon 8 (931bp) skipping will shift the exon 10 reading frame, substituting 30 different AA for the 354 AA tail of the normal "long" mGluR1α isoform. The normal "short" mGluR1 β1 isoform will be replaced by a hybrid molecule, where 28 different AA are encoded by exon 9, the reading frame is restored and the 308 AA encoded by exon 10 are added. Transcripts ending in intron 8 are predicted to encode a truncated protein, where the RRKK amino acid sequence is exposed. LBD – ligand-binding domain; CRD – cysteine-rich domain; 7TM – 7 transmembrane domain.

Table S1. **Proportion of Alleles Estimated to be Shared Identical by Descent (IBD) between Each Pairwise Combination of the 11 Individuals Sequenced**

Pairs of Individuals		Estimated Proportion of SNPs at which 0, 1, or 2 Alleles are Shared IBD			Overall Proportion of SNPs Shared IBD	
Person 1	**Person 2**	**0**	**1**	**2**	**Observed**	**Expected**
V2-1	V2-2	1	0	0	0	0
V2-2	V3-2	0	1	0	0.5	0.5
V2-2	V3-1	0	1	0	0.5	0.5
V2-1	V3-2	0	1	0	0.5	0.5
V2-1	V3-1	0	1	0	0.5	0.5
V3-1	V3-2	0.2881	0.5281	0.1838	0.4478	0.5
M1-1	M2-2	0	1	0	0.5	0.5
M1-1	M2-1	0	1	0	0.5	0.5
M2-1	M2-2	0.3125	0.3999	0.2877	0.4876	0.5
B3-4	B4-2	0	1	0	0.5	0.5
B3-3	B4-3	0	1	0	0.5	0.5156
B4-2	B4-3	0.8286	0.1714	0	0.0857	0.1367
B3-3	B4-2	0.9542	0.0458	0	0.0229	0.0313
B3-4	B4-3	1	0	0	0	0
B3-3	B3-4	1	0	0	0	0
All inter-family pairs		1	0	0	0	0

Expected values are conditional on reported inbreeding.

Table S2. **Estimated Inbreeding Coefficients (F) and Their Standard Errors for the 11 Individuals Included in Exome Sequencing**

Individual	Estimated Inbreeding Coefficient (F)	Standard Error
B3-3	0.075	0.014
B3-4	0.071	0.014
B4-2	0.104	0.014
B4-3	0.089	0.020
M1-1	0.088	0.017
M2-1	0.113	0.017
M2-2	0.091	0.015
V2-1	0.081	0.014
V2-2	0.000	0.000
V3-1	0.023	0.011
V3-2	0.035	0.012

For comparison, the expected F values for the offspring of double first cousins, first cousins, first cousins once removed, or half-cousins and second cousins, are 0.125, 0.063, 0.031 and 0.016 respectively. B4-3 is known to be the offspring of half-first cousins; no other inbreeding loops were reported.

Table S3. Animal Models with Mutations in *Grm1*

Name	Mutation	Manifestations									Ref
		Onset	Body Size	Gross Cerebellar Anatomy	Ataxia	Intention Tremor	Learning Deficits	Eyes	BAEPs	Other	
Grm1^{tm1Stl}	Knockout			Normal	Yes	Yes	Context-specific associative; motor	Abnormal eyeblink conditioning			1
Grm1^{tm1Crpl}	Knockout	2-3w	Small	Normal	Yes	Yes	Spatial learning			Pre-pulse inhibition deficit	2
Grm1^{tm1Dgen}	Knockout	3w	Small	Normal	Yes					Low bone mineral density	Jackson Lab Database
Crv4	190bp ins, fsh	At walking	Small	Normal	Yes	Yes		"More closed"		Increased brown fat; Kyphoscoliosis	3
Grm1^{wobl}	W320L	At weaning			Yes					Low fertility	4
Grm1^{nmf373}	I160T	3w		Normal	Yes	Yes					4
Grm1^{rcw}	E292D	"Early"		Normal	Yes						4
Grm1^{rcw2J}	DupEx4	"Early"	Small	Normal	Yes						4
Grm1$^{rcw3J\ and\ 4J}$	G337E	2w	Small	Normal	Yes				Increased latencies		4
Bandera (Coton de Toulear dogs)	62bp ins, Exon8, fsh	2w	Normal	Normal	Yes	Yes		Absent menace response; Saccadic dysmetria	Normal		5

Ins – insertion; Fsh – frame shift; w – weeks; BAEPs – brainstem auditory evoked potentials; Ref - reference

References used in Table S3

1. Aiba, A., Kano, M., Chen, C., Stanton, M.E., Fox, G.D., Herrup, K., Zwingman, T.A., and Tonegawa, S. (1994). Deficient cerebellar long-term depression and impaired motor learning in mGluR1 mutant mice. Cell 79, 377-388.

2. Conquet, F., Bashir, Z.I., Davies, C.H., Daniel, H., Ferraguti, F., Bordi, F., Franz-Bacon, K., Reggiani, A., Matarese, V., Conde, F., et al. (1994). Motor deficit and impairment of synaptic plasticity in mice lacking mGluR1. Nature 372, 237-243.

3. Conti, V., Aghaie, A., Cilli, M., Martin, N., Caridi, G., Musante, L., Candiano, G., Castagna, M., Fairen, A., Ravazzolo, R., et al. (2006). crv4, a mouse model for human ataxia associated with kyphoscoliosis caused by an mRNA splicing mutation of the metabotropic glutamate receptor 1 (Grm1). Int. J. Mol. Med. 18, 593-600.

4. Sachs, A.J., Schwendinger, J.K., Yang, A.W., Haider, N.B., and Nystuen, A.M. (2007). The mouse mutants recoil wobbler and nmf373 represent a series of Grm1 mutations. Mamm. Genome 18, 749-756.

5. Coates, J.R., O'Brien, D.P., Kline, K.L., Storts, R.W., Johnson, G.C., Shelton, G.D., Patterson, E.E., and Abbott, L.C. (2002). Neonatal cerebellar ataxia in Coton de Tulear dogs. J. Vet. Intern. Med. 16, 680-689.

Table S4. Primers Used in RT-PCR and qPCR Analyses of *GRM1* Transcripts

Amplicon	Primer Sequence	hg19 Start Position	hg19 End Position	Expected Product Size (bp)	
				α	β1
exon 3-4 RT-PCR	GGAGAAGAGCTTTGACCGACT	146480581	146480601	304	
	ACCAGGGATTCCTCGTGTTAG	146625878	146625898		
exon 3-4 qPCR	CTGCTTCTGTGAAGGCATGA	146480647	146480666	108	
	ATCTCTGTCTGCCCATCCAT	146625749	146625768		
exon 7-10 RT-PCR	AGATGAGTTCACCTGCAAAGC	146708094	146708114	1,030	1,115
	CTCCACCTGGTTCAGACCAT	146755029	146755048		
	GTGCCTTCACCACCTCTGAT	146720718	146720737	Nested (exon 8) forward sequencing primer	
exon 7-IVS 8 RT-PCR	CCTGCAAAGAGAATGAATATGTGC	146708069	146708092	1,144	
	GGGGAAATGGAAGAGACAAC	146720946	146720965		
	ACTATGCCTTCAAGACCCGC	146720481	146720500	Nested (exon 8) forward sequencing primer	
exon 7-IVS 7 control PCR	CCTGCAAAGAGAATGAATATGTGC	146708069	146708092	231 in genomic DNA; no cDNA product expected	
	TTATGTATACTCCTTGACATGAGGAC	146708275	146708300		

Reverse transcription (RT)-PCR

Lymphoblastoid cell lines (LCLs) were established using standard protocols for EBV transformation and culture conditions (37°C/5%CO_2 in advanced RPMI, supplemented with Glutamax, 20% foetal calf serum and 100U/ml Penicillin/Streptomycin). Total RNA was extracted using RNeasy Plus Mini kit from ~6X10^6 cells homogenized with QIAshredder columns and treated with RNAse-Free DNAse (reagents from QIAGEN, Doncaster, Vic, Australia). Four µg total RNA per sample were used for cDNA synthesis by the SuperScript III First-Strand Synthesis System (Life Technologies, Mulgrave, Vic, Australia). Positive controls included HeLa total RNA (provided with the kit) and human brain total RNA (Clontech, Mountain View, CA, USA), and RNAse-free water served as a negative control. Prior to PCR, cDNA products were diluted 1:10 in nuclease-free water (1:100 for brain cDNA). *GRM1* RT-PCR was carried out in 24 µl reactions, containing 4 µl cDNA, 0.6 µM primers, 5% DMSO, and 1X KAPA Taq ReadyMix (Kapa Biosystems, Woburn, CA, USA). Reaction conditions were as described, [40(main text)]) with initial denaturation at 95°C for 2 min, 10 cycles of denaturation at 94°C for 20 sec, annealing at 64°C for 15 sec with a touch down 0.5°C/cycle, and extension at 72°C for 1 min, 44 cycles of denaturation at 94°C for 20 sec, annealing at 59°C for 15 sec, and extension at 72°C for 1 min, and final extension at 72°C for 5 min.

Quantitative PCR

qPCR was carried out in 10 µl reactions containing 4 µl test cDNA or standard, 0.25 µM primers and 1X iQ SYBR Green Supermix (BioRad, Gladesville, NSW, Australia). All reactions were run in triplicates on an iQ5 real-time PCR detection system (BioRad) using initial denaturation at 95°C for 3 min, 50 cycles of denaturation at 95°C for 15 sec, and annealing/extension at 60°C for 60 sec, and final melting curve analysis.

Table S5. Comparison of the Clinical Features of Several Autosomal-Recessive Congenital Ataxias

Disorder	***GRM1* ataxia**	**CAMRQ1**	**CAMRQ2**	**CAMRQ3**	**Cayman ataxia**	**SCAR2**	**SCAR5**	**SCAR6**
MIM		224050	610185	613227	601238	213200	606937	608029
Gene / locus	*GRM1* / 6q24	*VLDLR* / 9p24.2	17p13	*CA8* / 8q12.1	*ATCAY* / 19p13.3	9q34-qter	*ZNF592* /15q25.3	20q11-q13
Congenital onset, developmental delay	+	+	+	+	+	+	+	+
	Cerebellar signs							
Gait ataxia	+	+	+	+	+	+	+	+
Dysdiadochokinesia	+/-	+/-	+	n.r.	n.r.	n.r.	+	n.r.
Dysmetria	+/-	+/-	+	n.r.	n.r.	+	+	n.r.
Intention tremor	+/-	+/-	+	+	+	+	-	+
Dysarthria	+	+	+	+	+	+	+	n.r.
Nystagmus	+/-	+	n.r.	n.r.	+	n.r.	+/-	+
Mental retardation	+	+	+	+	+	+	+	Delayed speech
Oculomotor abnormalities	+	+/- strabismus	+ strabismus	+/- strabismus	n.r.	+ strabismus	+/- esotropia, apraxia	n.r.
Pyramidal signs	+	+	-	-	n.r.	+/-	+	+
Short stature	+	+/-	+	n.r.	n.r.	+	+	+
Muscle hypotonia	+	+	+	n.r.	+	+	-	+
Pes planus	+	+	n.r.	n.r.	n.r.	+	n.r.	+
Additional features	Epilepsy Poly-neuropathy	Epilepsy	Epilepsy Dystonia	n.r.	n.r.	Microcephaly Cataracts	Optic nerve atrophy Skin abnormalities Microcephaly	n.r.
References	This study	1-4	5	6	7, 8	9, 10	11-13	14, 15

CAMRQ - cerebellar ataxia, mental retardation and dysequilibrium syndrome; SCAR - autosomal recessive spinocerebellar ataxia; +/- present in some patients; n.r. - not reported

References used in Table S5

1. Boycott, K. M., Flavelle, S., Bureau, A., Glass, H. C., Fujiwara, T. M., Wirrell, E., Davey, K., Chudley, A. E., Scott, J. N., McLeod, D. R., Parboosingh, J. S. (2005). Homozygous deletion of the very low density lipoprotein receptor gene causes autosomal recessive cerebellar hypoplasia with cerebral gyral simplification. Am. J. Hum. Genet. *77*, 477-483.
2. Tan, U. (2008). Unertan syndrome: review and report of four new cases. Int. J. Neurosci. *118*, 211-225.
3. Turkmen, S., Hoffmann, K., Demirhan, O., Aruoba, D., Humphrey, N., Mundlos, S. (2008). Cerebellar hypoplasia, with quadrupedal locomotion, caused by mutations in the very low-density lipoprotein receptor gene. Europ. J. Hum. Genet. *16*, 1070-1074.
4. Moheb, L. A., Tzschach, A., Garshasbi, M., Kahrizi, K., Darvish, H., Heshmati, Y., Kordi, A., Najmabadi, H., Ropers, H. H., Kuss, A. W. (2008). Identification of a nonsense mutation in the very low-density lipoprotein receptor gene (VLDLR) in an Iranian family with dysequilibrium syndrome. Europ. J. Hum. Genet. *16*, 270-273.
5. Turkmen, S., Demirhan, O., Hoffmann, K., Diers, A., Zimmer, C., Sperling, K., Mundlos, S. (2006). Cerebellar hypoplasia and quadrupedal locomotion in humans as a recessive trait mapping to chromosome 17p. J. Med. Genet. *43*, 461-464.
6. Turkmen, S., Guo, G., Garshasbi, M., Hoffmann, K., Alshalah, A. J., Mischung, C., Kuss, A., Humphrey, N., Mundlos, S., Robinson, P. N. (2009). CA8 mutations cause a novel syndrome characterized by ataxia and mild mental retardation with predisposition to quadrupedal gait. PLoS Genet. *5*, e1000487.
7. Nystuen, A., Benke, P. J., Merren, J., Stone, E. M., Sheffield, V. C. (1996). A cerebellar ataxia locus identified by DNA pooling to search for linkage disequilibrium in an isolated population from the Cayman Islands. Hum. Mol. Genet. *5*, 525-531.
8. Bomar, J. M., Benke, P. J., Slattery, E. L., Puttagunta, R., Taylor, L. P., Seong, E., Nystuen, A., Chen, W., Albin, R. L., Patel, P. D., et al. (2003). Mutations in a novel gene encoding a CRAL-TRIO domain cause human Cayman ataxia and ataxia/dystonia in the jittery mouse. Nature Genet. *35*, 264-269.
9. Megarbane, A., Delague, V., Salem, N., Loiselet, J. (1999). Autosomal recessive congenital cerebellar hypoplasia and short stature in a large inbred family. Am. J. Med. Genet. *87*, 88-90.
10. Delague, V., Bareil, C., Bouvagnet, P., Salem, N., Chouery, E., Loiselet, J., Megarbane, A., Claustres, M. (2001). Nonprogressive autosomal recessive ataxia maps to chromosome 9q34-9qter in a large consanguineous Lebanese family. Ann. Neurol. *50*, 250-253.
11. Megarbane, A., Delague, V., Ruchoux, M. M., Rizkallah, E., Maurage, C. A., Viollet, L., Rouaix-Emery, N., Urtizberea, A. (2001). New autosomal recessive cerebellar ataxia disorder in a large inbred Lebanese family. Am. J. Med. Genet. *101*, 135-141.
12. Delague, V., Bareil, C., Bouvagnet, P., Salem, N., Chouery, E., Loiselet, J., Megarbane, A., Claustres, M. (2002). A new autosomal recessive non-progressive congenital cerebellar ataxia associated with mental retardation, optic atrophy, and skin abnormalities (CAMOS) maps to chromosome 15q24-q26 in a large consanguineous Lebanese Druze family. Neurogenetics *4*, 23-27.
13. Nicolas, E., Poitelon, Y., Chouery, E., Salem, N., Levy, N., Megarbane, A., Delague, V. (2010). CAMOS, a nonprogressive, autosomal recessive, congenital cerebellar ataxia, is caused by a mutant zinc-finger protein, ZNF592. Europ. J. Hum. Genet. *18*, 1107-1113.
14. Kvistad, P. H., Dahl, A., Skre, H. (1985). Autosomal recessive non-progressive ataxia with an early childhood debut. Acta Neurol. Scand. *71*, 295-302.
15. Tranebjaerg, L., Teslovich, T. M., Jones, M., Barmada, M. M., Fagerheim, T., Dahl, A., Escolar, D. M., Trent, J. M., Gillanders, E. M., Stephan, D. A. (2003). Genome-wide homozygosity mapping localizes a gene for autosomal recessive non-progressive infantile ataxia to 20q11-q13. Hum. Genet. *113*, 293-295.